J Mater Sci (2017) 52:10787–10799

Chemical routes to materials

Effects of additives on sucrose-derived activated carbon microspheres synthesized by hydrothermal carbonization

Haiyang Zhao[1], Xiaoai Lu[1], Yue Wang[1], Bin Sun[1], Xianghao Wu[1], and Hanfeng Lu[1,*]

[1] *Research Institute of Catalytic Reaction Engineering, College of Chemical Engineering, Zhejiang University of Technology, Hangzhou 310014, China*

Received: 21 February 2017
Accepted: 1 June 2017
Published online: 7 June 2017

ABSTRACT

In the hydrothermal carbonization of carbohydrates, such as sucrose as raw material in this study, activated carbon microspheres were synthesized by two steps of hydrothermal carbonization (180 °C) and further heat treatment in nitrogen (1000 °C). The main purpose of this study was to investigate the effects of additives, such as H_3PO_4, $ZnCl_2$, $SnCl_2$, and $CaCl_2$, on the surface characteristics and toluene adsorption ability by adding them into the two processes. The structural, chemical, and adsorption properties of sucrose-derived activated carbon microspheres were characterized using nitrogen adsorption, scanning electron microscopy, X-ray diffraction, Fourier transform infrared spectroscopy, water contact angles, and dynamic adsorption of toluene. Results showed that additives played important roles in the synthesis process. The addition of $CaCl_2$ in the hydrothermal process, the specific surface area of activated carbon spheres increased up to 1180 $m^2\ g^{-1}$ compared with that of the blank sample (i.e., 724 $m^2\ g^{-1}$). By contrast, the addition of H_3PO_4 in the heat treatment process increased the specific surface area to 1529 $m^2\ g^{-1}$. Moreover, the micromorphology of activated carbon microspheres was more homogeneous when additives were added in the heat treatment process, but the activated carbon microspheres were more hydrophobic when additives were added in the hydrothermal process. These findings may help researchers to understand the influence of additives on the preparation of hydrochar-derived activated carbon.

Introduction

Biomass plays an important role in sustainable development because of its large reserves and renewability. In addition to being a food source and renewable raw materials, it can also be used for the production of energy, carbon sequestration, and preparation of hydrochar and activated carbon (AC) [1].

Address correspondence to E-mail: luhf@zjut.edu.cn

DOI 10.1007/s10853-017-1258-4

In recent years, the conversion of biomass into valuable carbon materials by hydrothermal carbonization (HTC) [2–12] had become the focus of many researchers because of its mild reaction conditions, simple operation, low cost, water as solvent without the need for organic solvent, high carbon yield, as well as the hydrochar produced with less ash, and more surface containing oxygen functional groups [13]. In the HTC process, the carbohydrate components in the biomass that is hydrolyzed, dehydrated, and dissolved in water, followed by a series of aldol reaction, cycloaddition reaction, and condensation, finally a carbon-rich solid product was obtained, namely hydrochar [7, 14].

However, hydrochar has a less aromatic structure, poor thermal stability, a low specific surface area, and underdeveloped porosity, which limit the exploitation of hydrochar for practical applications [15]. Therefore, methods to improve the yield of hydrothermal carbon materials, surface area, and porosity are necessary. A number of studies have been conducted using catalysts for biomass decomposition under hydrothermal condition, either to enhance the reaction rate or to tailor the path of reaction for the conversion of biomass into specific products [3–6, 16–20]. Recently, Quesada-Plata et al. [21] investigated the ACs prepared through H_3PO_4-assisted HTC from biomass wastes, and ACs of surface areas above 2000 $m^2\ g^{-1}$ and tunable pore size distribution had been obtained. Several studies have been conducted using hydrochar as a precursor to prepare AC with well-developed porosity by subsequent physical activation or chemical activation [8, 14, 22–24]. Jain et al. [23, 25, 26] reported hydrothermal pre-treatment of coconut shell in the presence of $ZnCl_2$ to improve chemical activation and show a significant improvement in mesoporous area by as much as 80%.

As a typical representative of the biomass, carbohydrates, such as glucose [11, 17, 27–29], fructose [28], lactose [29], sucrose [24, 27], starch [6, 22, 27], and cellulose [10, 11, 13, 16], which are low in price and rich in nature reserves, have been extensively studied to synthesize hydrochar by HTC as a carbon source. In 2001, Wang et al. [30] first reported the synthesis of carbon spherules with tunable size (in the 0.25–5 μm range) by HTC of sucrose at 190 °C through regulating the concentration of the sucrose solution and the dwell time. Afterward, Sevilla et al. [10, 27, 31] investigated the HTC of different saccharides (glucose, sucrose, starch, and cellulose) and proposed the mechanism of hydrochar formation and oxygen functional groups (OFGs) based on the nucleation model described by Mer [32]. Some time ago, Zhang et al. [33] reported that using NH_4Cl additive for HTC of glucose, and after following KOH activation, N-doped highly porous carbon with high specific surface area (exceeding 3000 $m^2\ g^{-1}$) was obtained, which was really an efficient route.

Thus far, most studies focused on using sucrose as carbon source to prepare hydrochar, and some also investigated its further processing to prepare AC [24, 30, 34]. The easiest approach for the preparation of AC by hydrochar as precursors is thermal treatment under an inert atmosphere [15, 35]; however, adding small amount of additives in the HTC process or subsequent heat treatment process to improve the quality of carbon materials is rarely studied; additives may play a huge effect on the HTC or heat treatment.

In this sense, the main objective of this work is to hydrothermally synthesize the carbon microspheres by using sucrose as carbon source and subsequently performing heat treatment to develop porosity into AC microspheres. Meanwhile, the influence of four additives (H_3PO_4, $ZnCl_2$, $SnCl_2$, and $CaCl_2$) on the properties (such as pore structure, surface area, surface morphology, and toluene adsorption capacity) of AC microspheres was explored by adding a small amount of these additives in the hydrothermal process or heat treatment process. Moreover, the mechanism of the additives was also discussed.

Materials and methods

Preparation of carbon microspheres

A typical synthesis was conducted as follows: Sucrose (6 g) was dissolved in 50 mL of distilled water and stirred until completely dissolved. The solution was then sealed into a 100-mL Teflon-lined stainless steel autoclave. The synthesis was conducted in a pre-heated furnace at 180 °C for 24 h. Afterward, the autoclave was naturally cooled down to room temperature, the obtained solid samples were washed with distilled water and ethanol thrice to remove the soluble residues and then placed in a dry box at 110 °C for 2 h, and the hydrochar materials were obtained. The as-prepared hydrochar

materials were further heated at 1000 °C (with heating rate of 10 °C min^{-1}) for 2 h under N_2 atmosphere (N_2 flow rate was 200 mL min^{-1}) in a quartz tube furnace. After cooling to room temperature, hydrochar materials were washed with distilled water thrice and dried at 110 °C for 6 h, and AC samples were obtained; these are the blank samples. For the addition during the hydrothermal process, 6 g of sucrose and 1.5 g of additives were dissolved in distilled water together before the hydrothermal treatment. However, for the addition during the heat treatment process, the hydrochar from 6 g of sucrose and 1.5 g of additive was mixed uniformly before heat treatment. The preparation process of AC is illustrated in Fig. 1.

The hydrothermal process of sucrose represented by HT and P, Zn, Sn, and Ca represented by H_3PO_4, $ZnCl_2$, $SnCl_2$, and $CaCl_2$, respectively. For example, adding H_3PO_4 in the hydrothermal process and then heat treatment was denoted as P-HT-1000, while sucrose hydrothermally treated individually and then heat-treated with H_3PO_4 was denoted as HT-P-1000.

Characterization

The physical characteristics of the carbon materials, including their specific surface area and pore volume, were measured by N_2 (g) adsorption in Micromeritics 3Flex micropore analyzer at 77 K in liquid N_2. Before the adsorption measurement, the samples were degassed at 280 °C for 6 h. Surface area was calculated according to Brunauer–Emmett–Teller method by using adsorption data acquired at a relative pressure (P/P_0) ranging from 0.05 to 0.25. The total pore volume was estimated based on the amount adsorbed at a relative pressure of approximately 0.995.

The XRD data of the samples were collected on a PANalytical X'Pert PRO X-ray diffractometer equipped with Ni-filtered Cu Kα ($\lambda = 0.1541$ nm, 40 kV) radiation. Measurements were taken within the 2θ range of 10°–80° with a step size of 0.02° s^{-1}.

Fourier transform infrared (FTIR) spectra were obtained by KBr method, recorded on a Bruker Vertex 70 infrared spectrometer, and scanned from 4000 to 500 cm^{-1}.

Scanning electron microscopy (SEM) images were acquired from Hitachi S4700 field emission scanning electron microscope with a field emission voltage of 15.0 kV. Before the test, the samples were sprayed with gold.

Transmission electron microscopy (TEM) images were acquired from Tecnai G2 F30 S-Twin high-resolution transmission electron microscope with testing acceleration voltage of 300 kV.

The water contact angles (WCA) of the samples were measured using theta optical tensiometer (KSV Instruments) and electro-optics with a closed-circuit television camera connected to a computer (Attension Theta software). Samples were placed on a sample stage, and a droplet of distilled water (2 or 5 μL) was deposited on the surface of the samples. A 2-μL water droplet could not stick on the surface of several samples. Consequently, the volume of the water droplet was increased to 5 μL. The WCA of each sample was measured thrice, and the average value was recorded.

Adsorption performance test

Toluene was used as a model. Gaseous toluene was generated by bubbling liquid toluene at 0 °C with nitrogen gas flow. The flow volume was regulated by a mass flow controller. The generated gaseous toluene was transferred to a buffer by N_2 stream and then diluted with N_2 at the required concentration. The total flow rate is 100 mL min^{-1}. The gaseous toluene was then passed through an adsorption column at 30 °C. The column (10 mm in diameter,

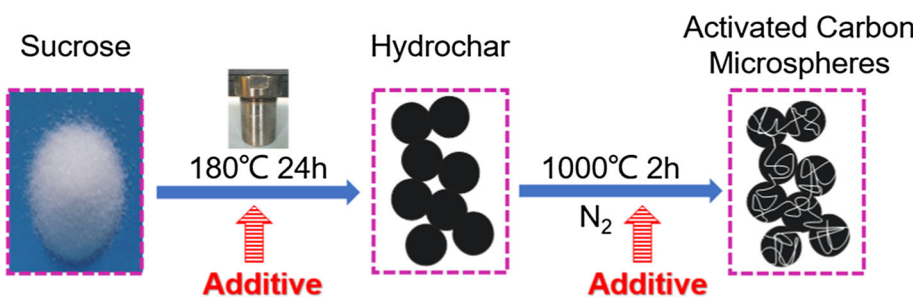

Figure 1 Schematic diagram of the preparation process of activated carbon microspheres.

200 mm in height) was packed with the as-prepared AC of approximately 0.3 g. The inlet and the outlet toluene concentrations were monitored online by Agilent 7890 gas chromatograph equipped with a flame ionization detector. The inlet toluene concentration was controlled at 8200 mg m^{-3}. Adsorption capacity was calculated according to Eq. (1):

$$q = \frac{F \times C_0 \times 10^{-9}}{W}\left[t_s - \int_0^{t_s} \frac{C_i}{C_0} dt\right] \quad (1)$$

where q is the equilibrium adsorption capacity (mg g^{-1}), F is the flow volume of the carrier gas (N_2) (100 mL min^{-1}), t_s is the time to reach adsorption equilibrium (min), W is the weight of the adsorbent (g), C_0 is the inlet concentration of the adsorbed gas (mg m^{-3}), and C_i is the outlet concentration of the adsorbed gas (mg m^{-3}).

Results and discussion

Characterization of hydrochar and AC microspheres

Influence of additives on yields and textural properties

Table 1 shows the yields of carbon materials; yields of the products were determined by Eqs. (2) and (3):

$$\text{hydrochar yield } \% = \frac{\text{amount of obtained solid after HTC (g)}}{\text{initial amount of sucrose (g)}} \quad (2)$$

$$\text{AC yield } \% = \frac{\text{amount of obtained solid after heat treatment (g)}}{\text{initial amount of sucrose (g)}}. \quad (3)$$

The mass fraction of carbon in the sucrose was 42.1%, which can be considered as the theoretical yield. As shown in Table 1, the yield of hydrochar was 36.5%, and the reduction of quality was due to the dehydration of sucrose under HTC conditions [36]. Moreover, the BET surface of hydrochar could not be presented, suggesting that it nearly had no pore structure, which is common for carbonaceous materials prepared from carbohydrates with hydrothermal methods [19, 29, 35]. This result may be because sucrose formed into organic polymer, such as hydrochar, after hydrolysis, polymerization, and aromatization; it did not cause pore formation in the process, and it may also be related to pore blockage [7, 15]. After heat treatment, the yield of HT-1000 declined to 17% because the hydrochar was further carbonized and dehydrated under high temperature, as well as produced volatile substances. In sharp contrast, the surface area of HT-1000 increased to 724 m^2 g^{-1}; the higher specific surface area resulted from the dehydration of hydrochar and the generation of volatiles, and small organic molecules were removed to generate porosity [15]; thus, heat treatment in N_2 atmosphere was effective for developing the porosity of hydrochar materials [36].

When additives were added in the hydrothermal process, the yield of P-HT-1000, Zn-HT-1000, and

Table 1 Textural properties of carbon materials prepared by hydrothermal carbonization of sucrose

Samples	Yield (%)	S^a_{total} (m^2 g^{-1})	S^b_{micro} (m^2 g^{-1})	V^c_{total} (cm^3 g^{-1})	V^d_{micro} (cm^3 g^{-1})	$D^e_{aver.}$ (nm)
HT	36.5	–[f]	–	–	–	–
HT-1000	17.0	724	678	0.317	0.317	1.75
P-HT-1000	8.0	985	851	0.447	0.431	1.81
Zn-HT-1000	16.0	792	772	0.365	0.365	1.85
Sn-HT-1000	17.8	488	305	0.309	0.163	2.53
Ca-HT-1000	8.3	1180	840	0.556	0.425	1.88
HT-P-1000	9.4	1529	402	0.791	0.222	2.07
HT-Zn-1000	10.7	1323	624	0.660	0.341	2.00
HT-Sn-1000	11.6	889	268	0.450	0.148	2.03
HT-Ca-1000	17.7	483	483	0.219	0.219	1.82

[a] Total specific surface area, [b] micropore specific surface area, [c] total pore volume, [d] micropore volume, [e] average pore diameter, [f] below the instrument measurement standard, the data were not given

Ca-HT-1000 further decreased, but the specific surface area increased, of which adding $CaCl_2$ was excellent, the surface area reached more than 1180 $m^2\ g^{-1}$, and the surface area of Sn-HT-1000 decreased. This result may be because H_3PO_4, $ZnCl_2$, and $CaCl_2$ played a catalytic role in the hydrothermal process and promoted the hydrolysis of sucrose and polymerization of organic matters, which resulted in hydrochar with better carbon skeleton, of which $CaCl_2$ is excellent, and $CaCl_2$ did not enter into the hydrochar finally, just acted as catalyst (elemental analysis of the hydrochar showed that the mass percent of Ca and Cl was 0.0148% and 0.0082%, respectively, suggested that additives were almost removed by washing).

Furthermore, when additives were added in the thermal treatment process, the yield of HT-P-1000, HT-Zn-1000, and HT-Sn-1000 decreased, the specific surface area also improved, of which adding H_3PO_4 was excellent, and the specific surface area was the largest that reached up to 1529 $m^2\ g^{-1}$. Moreover, the mesoporous volume and average pore diameter increased, while the surface area of HT-Ca-1000 declined. Results indicated that H_3PO_4, $ZnCl_2$, and $SnCl_2$ played a role of activation in the heat treatment process, and the effect of H_3PO_4 in the porosity development was excellent. Simultaneously, Table 1 shows the specific surface area of AC roughly inversely proportional to the carbon yield. That is, the specific surface area increased as the yield decreased, because the porosity developing process can be considered as an etching process in a certain range; the specific surface area and pore volume increased with increasing degree of etching. Afterward, it would consume more carbon, thus resulting in the decreased carbon yield.

The N_2 adsorption/desorption isotherms are exhibited in Fig. 2. According to the International Union of Pure and Applied Chemistry classification, the adsorption isotherm for HT-1000, P-HT-1000, Zn-HT-1000, Ca-HT-1000, and HT-Ca-1000 can be assigned to type I with obvious adsorption at a low relative pressure. The N_2 isotherms for Sn-HT-1000 belonged to the type IV, hysteresis loop was appeared, indicating the existence of mesoporous structures. While the N_2 isotherms for HT-P-1000, HT-Zn-1000, and HT-Sn-1000 were between type I and type II, they feature a mixture of high N_2 uptake at $P/P_0 < 0.05$ with continually increasing adsorption at higher P/P_0 (0.05–0.4) for developed mesopores; the mesopore may be produced by the restructuring of the carbon backbone during the high-temperature heat treatment process [36].

Influence of additives on morphology

Figure 3 shows SEM images of sucrose and as-prepared carbon materials. Sucrose transformed into carbon microspheres with a diameter of approximately 1–2 μm after hydrothermal carbonization, and after subsequent heat treatment, the diameter of HT-1000 was nearly the same as before. When additives were added in the hydrothermal process, P-HT-1000 formed the AC

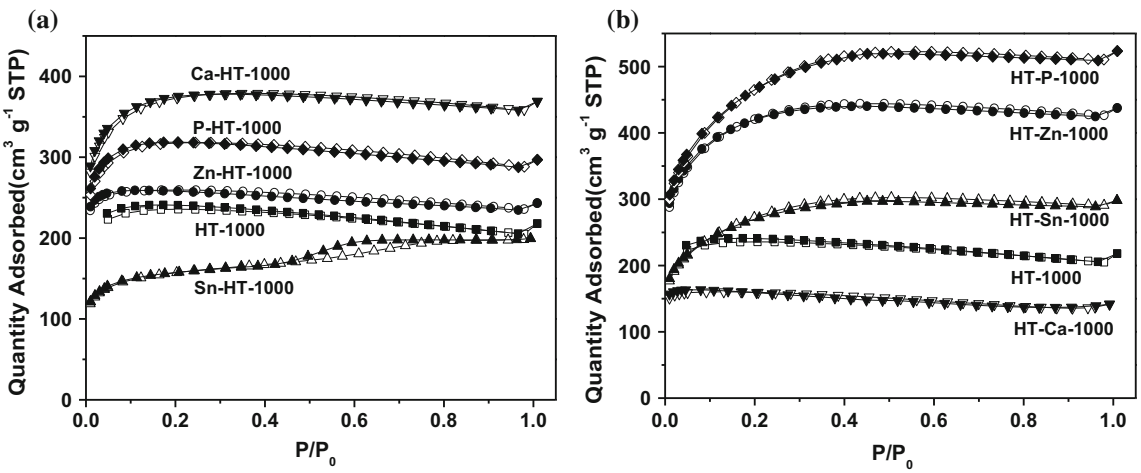

Figure 2 N_2 adsorption/desorption isotherms of **a** HT-1000 and activated carbons of added additives in the hydrothermal process and **b** HT-1000 and activated carbons of added additives in the heat treatment process.

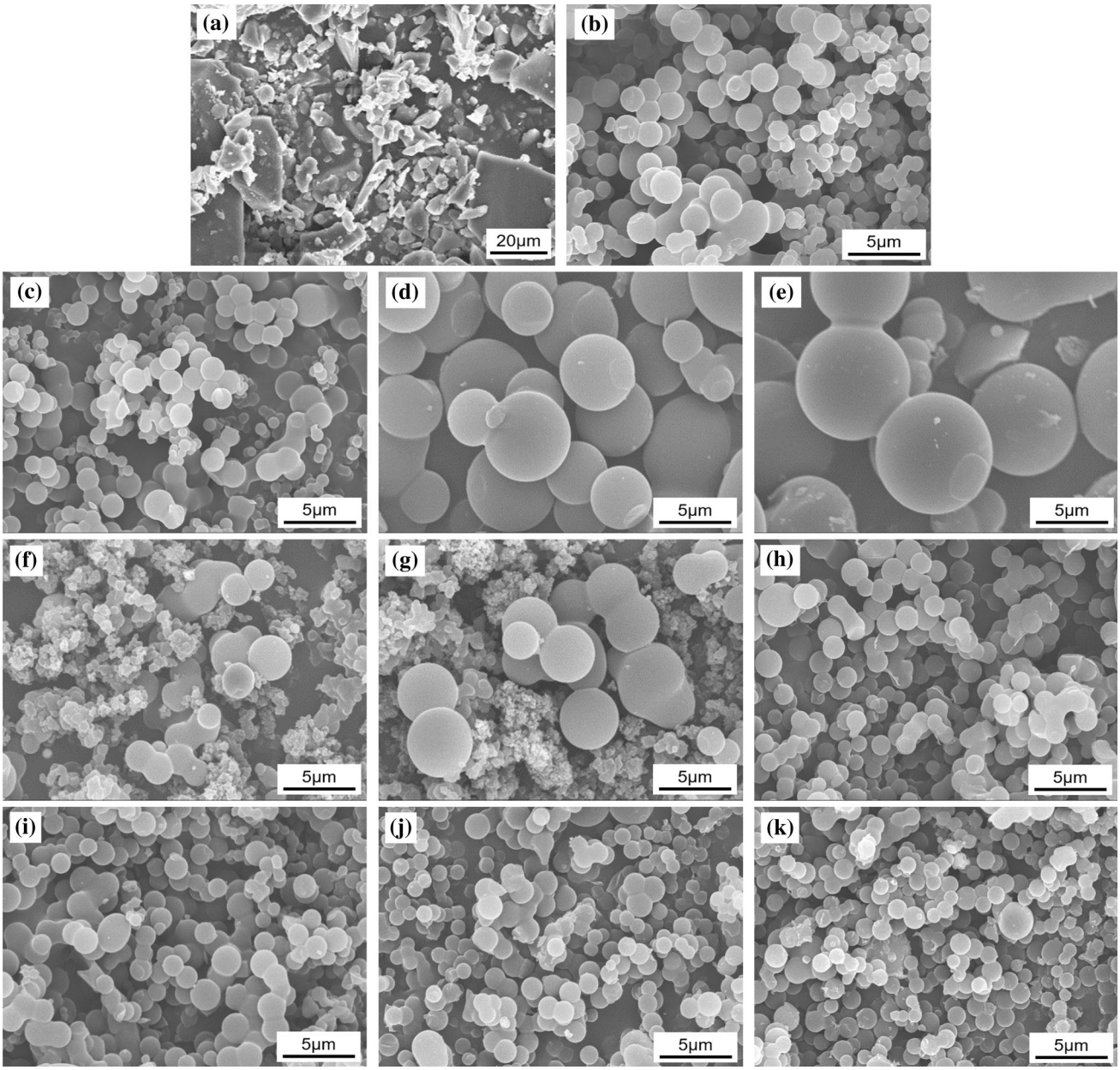

Figure 3 SEM images of **a** sucrose, **b** HT, **c** HT-1000, **d** P-HT-1000, **e** Zn-HT-1000, **f** Sn-HT-1000, **g** Ca-HT-1000, **h** HT-P-1000, **i** HT-Zn-1000, **j** HT-Sn-1000, **k** HT-Ca-1000.

microspheres with particle size ranging from 2 to 7 μm, and the particle size of Zn-HT-1000 was from 2 to 8 μm, while for Sn-HT-1000 and Ca-HT-1000, some were spherical structures, and some of which were coral structure. When additives were added in the heat treatment process, HT-P-1000, HT-Zn-1000, HT-Sn-1000, and HT-Ca-1000 all formed AC microspheres with uniform particle diameter of 1–1.5 μm, and the microspheres were basically similar to HT-1000.

Accordingly, the particle size of AC microspheres prepared by adding additives in the hydrothermal process was larger than that in the heat treatment process, which suggested that the kinetics of nucleation and growth in the particle formation process had changed when additives were added in the hydrothermal process. This result may be because the addition of additives in the hydrothermal process decreased the pH that can improve the formation of polymer, and the extension of the polymeric phase

and the progress of internal condensation are faster than the formation of spherical particles [3, 5]. However, according to the nucleation–growth mechanism following LaMer model, the strong acid prohibited some species with reactive oxygen functionalities (hydroxyl, carbonyl, carboxylic, etc.) from diffusing and linking to the nuclei and stopped the growth of carbon microsphere [22]. Lastly, it resulted in a distribution of shapes. Therefore, adding additives in the hydrothermal process was unfavorable to the formation of carbon spheres, which resulted in some carbon nuclei that could not grow into carbon spheres, while the addition of additives in the heat treatment process formed carbon microspheres with relatively homogeneous particle size and basically integrated shape.

TEM images of HT-1000 and HT-P-1000 samples as exampled in Fig. 4 also indicated that there were plenty of pore structures throughout the produced AC materials, and that HT-P-1000 had more pore structure than HT-1000, which was consistent with the results from BET.

XRD analysis

Figure 5 shows the XRD patterns of sucrose, HT, HT-1000, Ca-HT-1000, and HT-P-1000. As shown in the

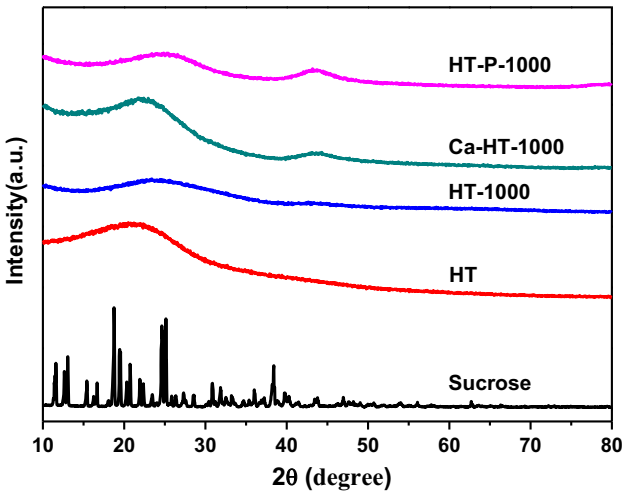

Figure 5 XRD patterns of sucrose, HT, HT-1000, Ca-HT-1000, and HT-P-1000.

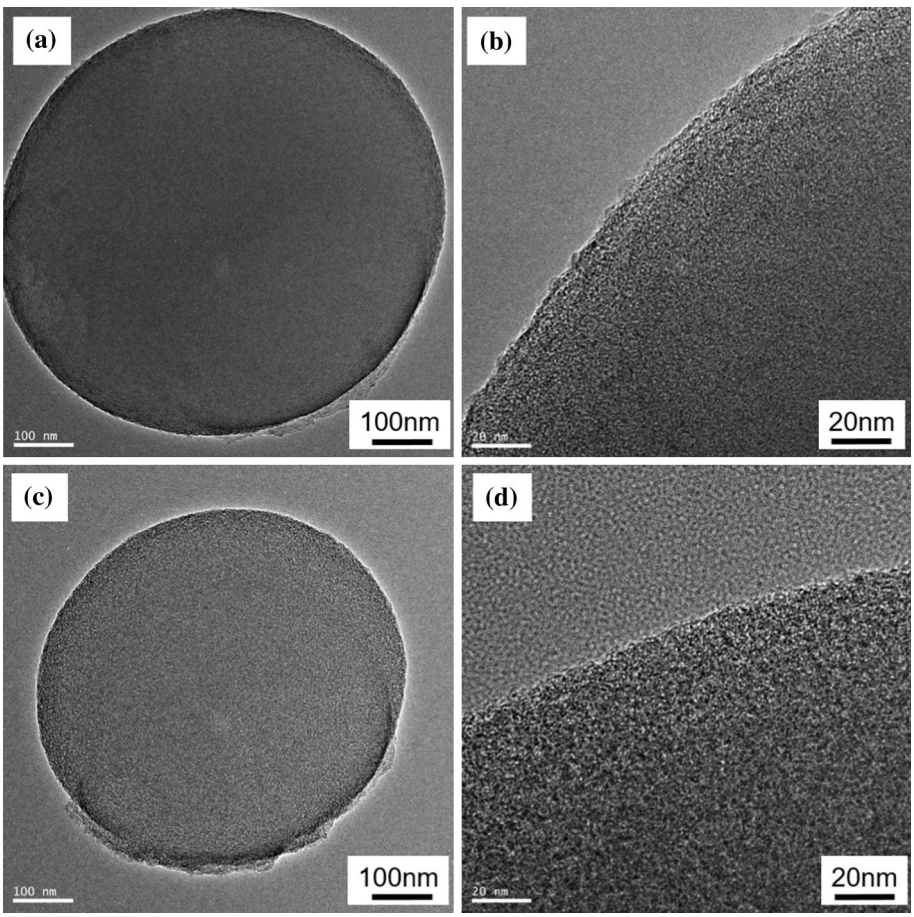

Figure 4 TEM images of **a**, **b** HT-1000, **c**, **d** HT-P-1000.

figure, the original crystal phase structure of sucrose was destroyed after hydrothermal treatment. All the carbon materials generated a broad diffraction peak around 24° and a weak diffraction peak around 44° in XRD patterns, which could be attributed to the (002) and (100) reflection of the graphitic-type lattice, indicating the formation of amorphous structures [36].

FTIR characterizations

The FTIR spectra of carbon spheres and sucrose starting material are shown in Fig. 6. For the HT sample, the broad band observed at 3000–3700 and 2900 cm^{-1} belongs to O–H (hydroxyl or carboxyl groups) and aliphatic C–H stretching vibration, respectively [27]. The bands at 1710 and 1620 cm^{-1} (together with the band at 1513 cm^{-1}) can be attributed to C=O (carbonyl, quinone, ester, or carboxyl) and C=C vibrations, respectively, whereas the bands in the 1000- to 1450-cm^{-1} region correspond to the C–O (hydroxyl, ester, and ether) stretching vibration and O–H bending vibration [7, 27]. The bands at 750–875 cm^{-1} are assigned to the out-of-plane bending vibration of the aromatic C–H [27]. All of these results suggest that after hydrothermal treatment of sucrose, surface functional groups of hydrochar become more abundant. A comparative analysis of the FTIR spectra of hydrochar and sucrose suggests that dehydration and aromatization processes occur during the hydrothermal carbonization. The intensities of the bands corresponding to the hydroxyl or carboxyl groups (3400 and 1000–1450 cm^{-1}) in the hydrochar are weaker than those of the corresponding sucrose, thereby suggesting that dehydration occurred [10]. The appearance of the bands at 1620 and 1513 cm^{-1} reveals the aromatization of the samples [10].

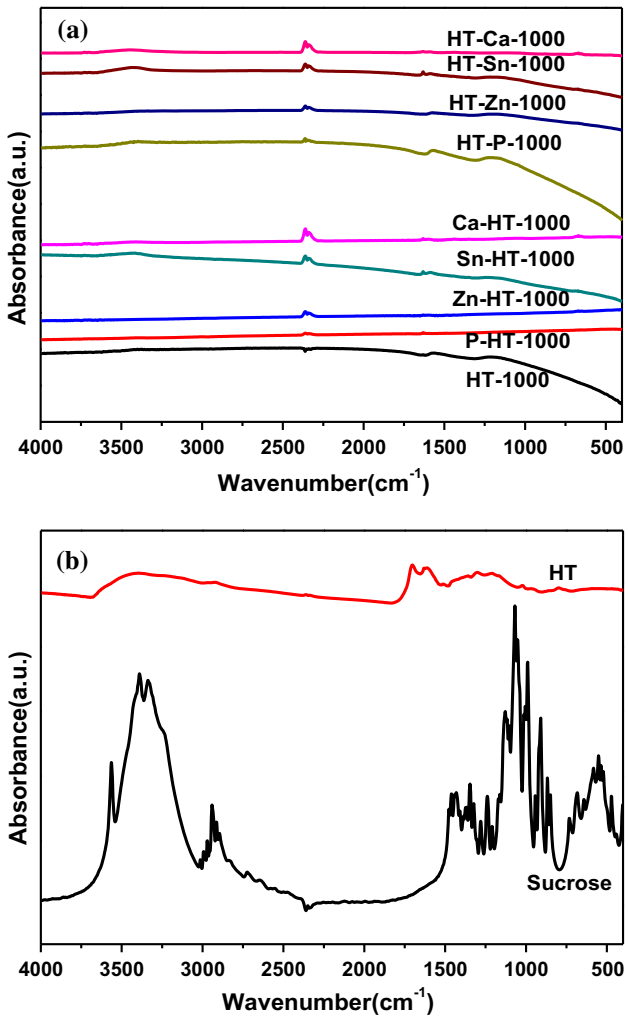

Figure 6 FTIR spectra of **a** activated carbon microspheres obtained by hydrothermal carbonization and further heat treatment of sucrose and **b** sucrose and HT.

When the hydrochar was heated at 1000 °C for 2 h, the number of vibration peaks reduced markedly and intensity significantly weakened, indicating a substantial reduction in the surface functional groups of AC. Only weak stretching vibration of O–H and C=C appeared at 3400 and 1620 cm^{-1}, respectively, weak C–O stretching vibration and O–H bending vibration in the 1000–1450 cm^{-1} region; these results are consistent with the results of Hao et al. [34]. The peak at approximately 2350 cm^{-1} is identified with asymmetric stretching vibration of atmospheric carbon dioxide [37]. The FTIR spectra indicated that the heat treatment would lead to further dehydration and release of surface functional groups (e.g., OH group) and structural rearrangement and leave the sp^2-bonded carbon backbone finally [36]. Furthermore, the O–H band intensity of AC microspheres prepared by adding additives in the hydrothermal process was weaker than that in the heat treatment process; this may be caused by the acidity of the solution that prohibited some species with reactive oxygen functionalities (hydroxyl, carbonyl, carboxylic, etc.) from diffusing and linking to the nuclei [22] and can be removed in the form of small organic molecules during the heat treatment.

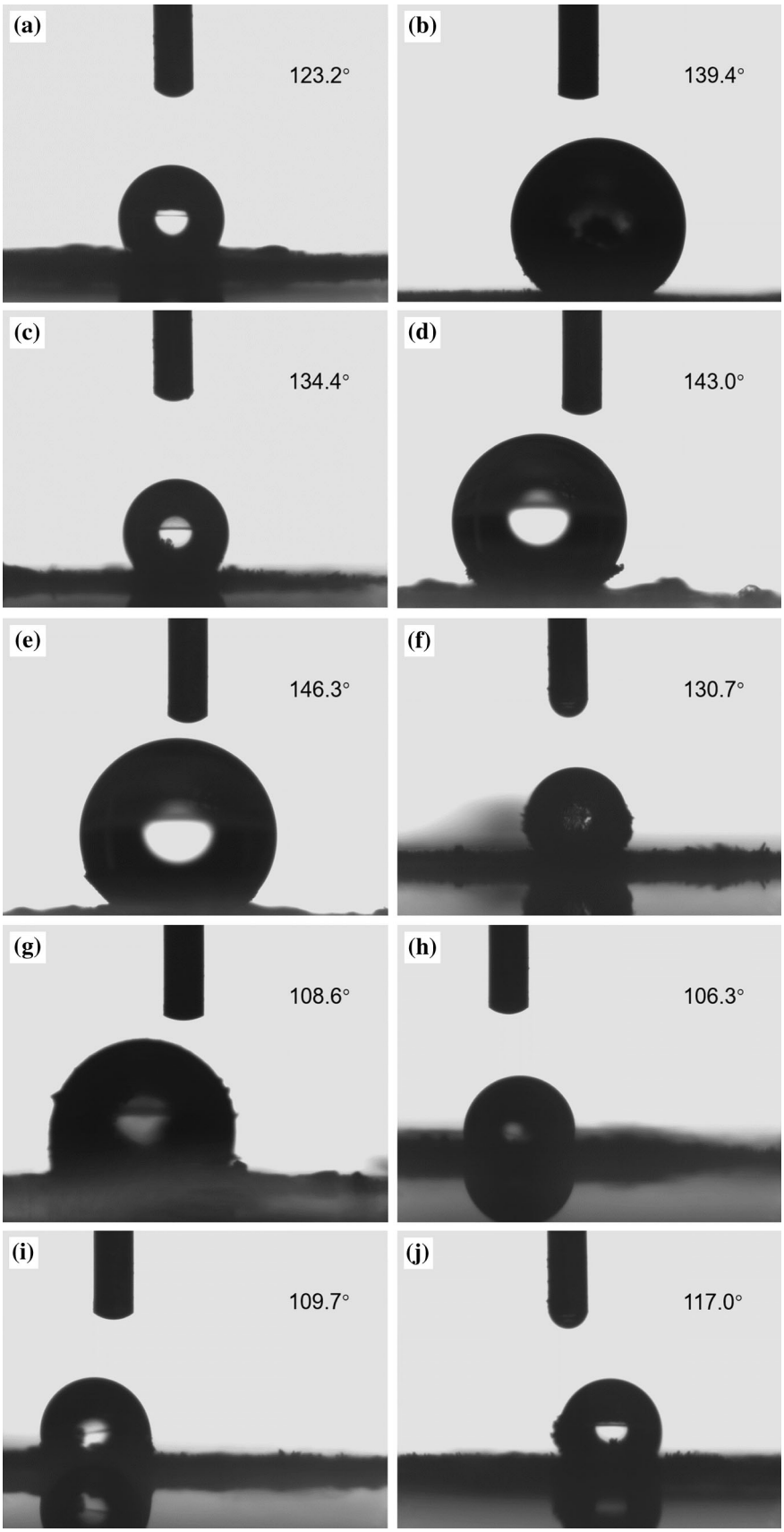

Figure 7 Photographs of a water droplet on a tablet of **a** HT, **b** HT-1000, **c** P-HT-1000, **d** Zn-HT-1000, **e** Sn-HT-1000, **f** Ca-HT-1000, **g** HT-P-1000, **h** HT-Zn-1000, **i** HT-Sn-1000, and **j** HT-Ca-1000.

WCA test

To identify the surface hydrophobic properties of the samples, the WCAs of the carbon materials were measured (Fig. 7). When a water droplet was allowed to contact with the surface of samples, the contact angle measured was all above 100°, suggesting that the carbon materials prepared by this method all performed good hydrophobicity. Moreover, from the results of contact angle measurements, P-HT-1000, Zn-HT-1000, Sn-HT-1000, and Ca-HT-1000 have a stronger hydrophobic nature than HT-P-1000, HT-Zn-1000, HT-Sn-1000, and HT-Ca-1000. This result is due to the amount of surface oxygen containing functional groups (e.g., OH group) of the latter that is more than the former, which was consistent with the observation from FTIR.

Dynamic adsorption

Figure 8 shows the toluene dynamic adsorption breakthrough curves of the AC samples. The curves can be divided into three stages. During the first stage, the toluene was almost completely adsorbed, and its outlet concentration was nearly zero. In the second stage, the toluene concentration gradually reached the breakthrough point (the outlet concentration was 5% of the inlet concentration), and the outlet concentration of toluene increased significantly with the increase in adsorption time. In the third stage, the outlet concentration increased in an S-shaped curve to the inlet concentration [38, 39]. As shown in the diagram, among all the samples, HT-P-1000 and Sn-HT-1000 exhibited the longest (i.e., reached 132 min) and the shortest (i.e., only 48 min) breakthrough times, respectively. Besides, the breakthrough time of HT-Zn-1000 was short but required a longer time to reach adsorption equilibrium. The need for an extended breakthrough time may be attributed to the existence of super-micropores in which the diameter was close to the toluene molecules, thereby increasing the diffusion resistance of toluene molecules from the outer to the inner micropores.

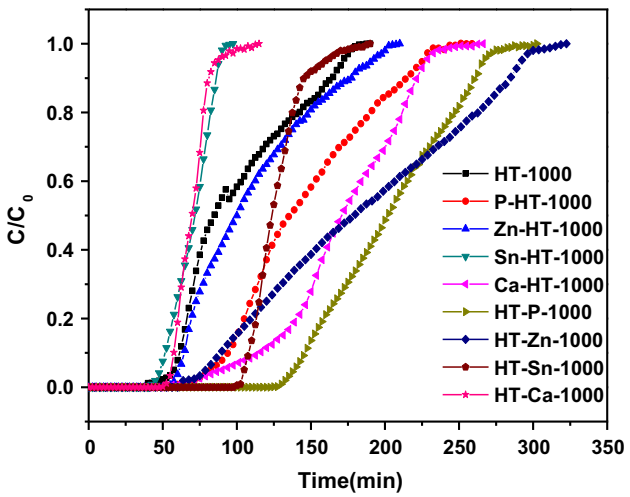

Figure 8 Experimental breakthrough curves of toluene on nine samples (GHSV: 20,000 mL h^{-1} g^{-1}, inlet toluene concentration 8200 mg g^{-1}).

As shown in Table 2, the saturated adsorption capacity of HT-1000 for toluene was 280.2 mg g^{-1}. When additives were added in the hydrothermal process, the saturated adsorption capacity of Ca-HT-1000 reached 460.6 mg g^{-1}, and when additives were added in the process of heat treatment, the saturated adsorption capacity of HT-P-1000 reached up to 548.3 mg g^{-1}, which was nearly two times greater than that of HT-1000. The adsorption capacity of all carbon materials at per square meter surface area was nearly equal, which suggested that the adsorption capacity of toluene was directly proportional to the specific surface area. That is, when specific surface area increased, the adsorption capacity of toluene increased correspondingly. Therefore, the presence of additives was necessary, and the addition of $CaCl_2$ in the hydrothermal process or the addition of H_3PO_4 in the heat treatment process could effectively improve the adsorption capacity of toluene on carbon spheres.

Mechanism of sucrose into carbon

Sucrose undergoes hydrolysis and formed glucose and fructose in the hydrothermal process; then, glucose, fructose, and other products of decomposition present in the solution undergo intermolecular dehydration and aldol condensation, which lead to polymerization. These polymers undergo aromatization, resulting in the formation of aromatic compounds; then, the formation of aromatic clusters occurs through intermolecular dehydration of aromatic compounds. These aromatic clusters will gather together to form a core when super-saturation state is reached in the aqueous solution; these nuclei develop based on nucleation model described by LaMer, then hydrochar spheres emerged [1]. After heat treatment in N_2 atmosphere, small organic

Table 2 Breakthrough characteristics of toluene adsorption onto activated carbon microspheres

Samples	Breakthrough time (min)	Saturated adsorption (mg g^{-1})	Breakthrough adsorption (mg g^{-1})	Adsorption per square meter (mg m^{-2})
HT-1000	56	280.2	156.4	0.3870
P-HT-1000	82	370.6	217.3	0.3762
Zn-HT-1000	61	298.1	166.1	0.3764
Sn-HT-1000	48	189.5	129.7	0.3883
Ca-HT-1000	90	460.6	240.3	0.3903
HT-P-1000	132	548.3	357.1	0.3586
HT-Zn-1000	79	528.6	227.8	0.3995
HT-Sn-1000	103	348.8	283.9	0.3924
HT-Ca-1000	54	189.2	146.1	0.3917

molecules are removed; porosity is generated within the hydrochar spheres, thereby forming the final AC microspheres. In this process, the hydrochar is actually a type of super-polymer with certain carbon skeleton, which is critical for the formation of porosity.

When additives were added in the hydrothermal process, $CaCl_2$ could promote carbon nuclei to form hydrochar with better carbon skeleton, but it also influenced the growth of carbon nucleus. Thus, it was unfavorable to the formation of carbon spheres, resulting in growing up of some carbon nuclei, while others could not. When additives were added in the heat treatment process, H_3PO_4 and $ZnCl_2$ had no influence on the formation of hydrochar spheres. Nevertheless, H_3PO_4 and $ZnCl_2$ as activation agents promoted the development of porosity. Consequently, AC microspheres with relatively uniform particle size and well-developed porosity were formed.

Conclusions

Sucrose was used as the carbon source, and hydrothermal method and further heat treatment were adopted to synthesize carbon microspheres. AC microspheres with high specific surface area and well-developed porosity were prepared by adding additives. From our findings, additives play significant roles in the synthesis process. When additives were added in the process of HTC in which $CaCl_2$ additive could play an effective role in promoting the formation of hydrochar with better carbon skeleton, the specific surface area of Ca-HT-1000 reached up to 1180 m^2 g^{-1} and adsorption capacity of toluene was 460.6 mg g^{-1}. While adding additives in the process of heat treatment, H_3PO_4 additive played a major role of activation in thermal processing, the specific surface area of HT-P-1000 was as high as 1529 m^2 g^{-1}, and adsorption capacity of toluene was up to 548.3 mg g^{-1}. On the contrary, adding additives in the hydrothermal process was unfavorable to the formation of carbon spheres, while the addition of additives in the thermal treatment process could form carbon microspheres with homogeneous particle size. These findings may help other researchers to understand the influence of additives on the preparation of hydrochar-derived AC.

Acknowledgements

We would like to acknowledge the financial support provided by the Natural Science Foundation of China (No. 21506194, 21676255) and Zhejiang Provincial Natural Science Foundation of China (No. Y14E080008, Y16B070025).

Compliance with ethical standards

Conflict of interest The authors declare that they have no conflict of interest.

References

[1] Jain A, Balasubramanian R, Srinivasan MP (2016) Hydrothermal conversion of biomass waste to activated carbon with high porosity: a review. Chem Eng J 283:789–805

[2] Donar YO, Çağlar E, Sınağ A (2016) Preparation and characterization of agricultural waste biomass based hydrochars. Fuel 183:366–372

[3] Lynam JG, Toufiq Reza M, Vasquez VR, Coronella CJ (2012) Effect of salt addition on hydrothermal carbonization of lignocellulosic biomass. Fuel 99:271–273

[4] Chen JZ, Chen ZH, Wang CH, Li XD (2012) Calcium-assisted hydrothermal carbonization of an alginate for the production of carbon microspheres with unique surface nanopores. Mater Lett 67:365–368

[5] Reiche S, Kowalew N, Schlögl R (2015) Influence of synthesis pH and oxidative strength of the catalyzing acid on the morphology and chemical structure of hydrothermal carbon. ChemPhysChem 16:579–587

[6] Supriya BS, Nagaraja P, Byrappa K (2015) Hydrothermal synthesis and characterization of carbon spheres using citric-acid-catalyzed carbonization of starch. e-Polymers 15:179–183

[7] Román S, Valente Nabais JM, Ledesma B, González JF, Laginhas C, Titirici MM (2013) Production of low-cost adsorbents with tunable surface chemistry by conjunction of hydrothermal carbonization and activation processes. Microporous Mesoporous Mater 165:127–133

[8] Pang LY, Zou B, Zou YC, Han X, Cao LY, Wang W, Guo YP (2016) A new route for the fabrication of corn starch-based porous carbon as electrochemical supercapacitor electrode material. Colloids Surf A 504:26–33

[9] Lynam JG, Coronella CJ, Yan W, Reza MT, Vasquez VR (2011) Acetic acid and lithium chloride effects on hydrothermal carbonization of lignocellulosic biomass. Bioresour Technol 102:6192–6199

[10] Sevilla M, Fuertes AB (2009) The production of carbon materials by hydrothermal carbonization of cellulose. Carbon 47:2281–2289

[11] Falco C, Baccile N, Titirici MM (2011) Morphological and structural differences between glucose, cellulose and lignocellulosic biomass derived hydrothermal carbons. Green Chem 13:3273–3281

[12] Titirici MM, Thomas A, Yu SH, Müller J, Antonietti M (2007) A direct synthesis of mesoporous carbons with bicontinuous pore morphology from crude plant material by hydrothermal carbonization. Chem Mater 19:4205–4212

[13] Kang SM, Li XL, Fan J, Chang J (2012) Characterization of hydrochars produced by hydrothermal carbonization of lignin, cellulose, D-xylose, and wood meal. Ind Eng Chem Res 51:9023–9031

[14] Wang LL, Guo YP, Zou B et al (2011) High surface area porous carbons prepared from hydrochars by phosphoric acid activation. Bioresour Technol 102:1947–1950

[15] Zhu XD, Liu YC, Zhou C, Luo G, Zhang SC, Chen JM (2014) A novel porous carbon derived from hydrothermal carbon for efficient adsorption of tetracycline. Carbon 77:627–636

[16] Zhao Y, Li W, Zhao X, Wang DP, Liu SX (2013) Carbon spheres obtained via citric acid catalysed hydrothermal carbonisation of cellulose. Mater Res Innov 17:546–551

[17] Cai HM, Lin XY, Tian LY, Luo XG (2016) One-step hydrothermal synthesis of carbonaceous spheres from glucose with an aluminum chloride catalyst and its adsorption characteristic for uranium(VI). Ind Eng Chem Res 55:9648–9656

[18] Takeuchi Y, Jin FM, Tohji K, Enomoto H (2008) Acid catalytic hydrothermal conversion of carbohydrate biomass into useful substances. J Mater Sci 43:2472–2475. doi:10.1007/s10853-007-2021-z

[19] Qi XH, Li LY, Tan TF, Chen WT, Smith RL Jr (2013) Adsorption of 1-butyl-3-methylimidazolium chloride ionic liquid by functional carbon microspheres from hydrothermal carbonization of cellulose. Environ Sci Technol 47:2792–2798

[20] Fechler N, Wohlgemuth SA, Jäker P, Antonietti M (2013) Salt and sugar: direct synthesis of high surface area carbon materials at low temperatures via hydrothermal carbonization of glucose under hypersaline conditions. J Mater Chem A 1:9418–9421

[21] Quesada-Plata F, Ruiz-Rosas R, Morallón E, Cazorla-Amorós D (2016) Activated carbons prepared through H_3PO_4-assisted hydrothermal carbonisation from biomass wastes: porous texture and electrochemical performance. ChemPlusChem 81:1349–1359

[22] Liang JL, Liu YH, Zhang J (2011) Effect of solution pH on the carbon microsphere synthesized by hydrothermal carbonization. Procedia Environ Sci 11:1322–1327

[23] Jain A, Aravindan V, Jayaraman S et al (2013) Activated carbons derived from coconut shells as high energy density cathode material for Li-ion capacitors. Sci Rep UK 3:3002

[24] Romero-Anaya AJ, Ouzzine M, Lillo-Ródenas M, Linares-Solano A (2014) Spherical carbons: synthesis, characterization and activation processes. Carbon 68:296–307

[25] Jain A, Balasubramanian R, Srinivasan MP (2015) Tuning hydrochar properties for enhanced mesopore development in activated carbon by hydrothermal carbonization. Microporous Mesoporous Mater 203:178–185

[26] Jain A, Jayaraman S, Balasubramanian R, Srinivasan MP (2014) Hydrothermal pre-treatment for mesoporous carbon synthesis: enhancement of chemical activation. J Mater Chem A 2:520–528

[27] Sevilla M, Fuertes AB (2009) Chemical and structural properties of carbonaceous products obtained by hydrothermal carbonization of saccharides. Chem A Eur J 15:4195–4203

[28] Yao CH, Shin YS, Wang LQ et al (2007) Hydrothermal dehydration of aqueous fructose solutions in a closed system. J Phys Chem C 111:15141–15145

[29] Aydıncak K, Tr Yumak, Sınağ A, Esen B (2012) Synthesis and characterization of carbonaceous materials from saccharides (glucose and lactose) and two waste biomasses by hydrothermal carbonization. Ind Eng Chem Res 51:9145–9152

[30] Wang Q, Li H, Chen LQ, Huang XJ (2001) Monodispersed hard carbon spherules with uniform nanopores. Carbon 39:2211–2214

[31] Sevilla M, Lota G, Fuertes AB (2007) Saccharide-based graphitic carbon nanocoils as supports for PtRu nanoparticles for methanol electrooxidation. J Power Sources 171:546–551

[32] Mer VKL (1952) Nucleation in phase transitions. Ind Eng Chem 44:1270–1277

[33] Zhang CY, Lin S, Peng JJ, Hong YZ, Wang ZY, Jin XB (2017) Preparation of highly porous carbon through activation of NH_4Cl induced hydrothermal microsphere derivation of glucose. RSC Adv 7:6486–6491

[34] Hao SW, Hsu CH, Liu YG, Chang BK (2016) Activated carbon derived from hydrothermal treatment of sucrose and its air filtration application. RSC Adv 6:109950–109959

[35] Titirici MM, White RJ, Falco C, Sevilla M (2012) Black perspectives for a green future: hydrothermal carbons for environment protection and energy storage. Energy Environ Sci 5:6796–6822

[36] Zhang PF, Zhang ZY, Chen JH, Dai S (2015) Ultrahigh surface area carbon from carbonated beverages: combining self-templating process and in situ activation. Carbon 93:39–47

[37] Li M, Cullen DA, Sasaki K, Marinkovic NS, More K, Adzic RR (2013) Ternary electrocatalysts for oxidizing ethanol to carbon dioxide: making ir capable of splitting C–C bond. J Am Chem Soc 135:132–141

[38] Zhang W, Qu Z, Li X, Wang Y, Ma D, Wu J (2012) Comparison of dynamic adsorption/desorption characteristics of toluene on different porous materials. J Environ Sci China 24:520–528

[39] Lu HF, Cao JJ, Zhou Y, Zhan DL, Chen YF (2013) Novel hydrophobic PDVB/R-SiO_2 for adsorption of volatile organic compounds from highly humid gas stream. J Hazard Mater 262:83–90